

REPORT DOCUMENTATION PAGE			Form Approved OMB NO. 0704-0188		
<p>The public reporting burden for this collection of information is estimated to average 1 hour per response, including the time for reviewing instructions, searching existing data sources, gathering and maintaining the data needed, and completing and reviewing the collection of information. Send comments regarding this burden estimate or any other aspect of this collection of information, including suggestions for reducing this burden, to Washington Headquarters Services, Directorate for Information Operations and Reports, 1215 Jefferson Davis Highway, Suite 1204, Arlington VA, 22202-4302. Respondents should be aware that notwithstanding any other provision of law, no person shall be subject to any penalty for failing to comply with a collection of information if it does not display a currently valid OMB control number.</p> <p>PLEASE DO NOT RETURN YOUR FORM TO THE ABOVE ADDRESS.</p>					
1. REPORT DATE (DD-MM-YYYY) 16-01-2011		2. REPORT TYPE Final Report		3. DATES COVERED (From - To) 1-Oct-2009 - 30-Jun-2010	
4. TITLE AND SUBTITLE Design of High-Performance Survival Radios using Discrete Time Analog Signal Processing			5a. CONTRACT NUMBER W911NF-09-1-0562		
			5b. GRANT NUMBER		
			5c. PROGRAM ELEMENT NUMBER 611102		
6. AUTHORS Ramesh Harjani			5d. PROJECT NUMBER		
			5e. TASK NUMBER		
			5f. WORK UNIT NUMBER		
7. PERFORMING ORGANIZATION NAMES AND ADDRESSES University of Minnesota - Minneapolis Sponsored Projects Administration 450 McNamara Alumni Center Minneapolis, MN 55455 -2009			8. PERFORMING ORGANIZATION REPORT NUMBER		
9. SPONSORING/MONITORING AGENCY NAME(S) AND ADDRESS(ES) U.S. Army Research Office P.O. Box 12211 Research Triangle Park, NC 27709-2211			10. SPONSOR/MONITOR'S ACRONYM(S) ARO		
			11. SPONSOR/MONITOR'S REPORT NUMBER(S) 57368-NS-II.1		
12. DISTRIBUTION AVAILABILITY STATEMENT Approved for Public Release; Distribution Unlimited					
13. SUPPLEMENTARY NOTES The views, opinions and/or findings contained in this report are those of the author(s) and should not be construed as an official Department of the Army position, policy or decision, unless so designated by other documentation.					
14. ABSTRACT In this project, we focused on the architectural and circuit-level design for a low cost, portable soldier radio with high survivability. We identified passive switched capacitor circuits as a suitable candidate for meeting these performance targets. We developed an architecture that uses a high dynamic range FFT to perform low amplitude signal detection in the presence of large jammers. Based on our analysis and modeling of non-idealities in switched capacitors, we were able to construct and simulate a sampled charge based 16 point FFT processor. The processor					
15. SUBJECT TERMS survival radio, wide-band, high dynamic range, FFT, analog signal processing, switched capacitors					
16. SECURITY CLASSIFICATION OF:			17. LIMITATION OF ABSTRACT UU	15. NUMBER OF PAGES	19a. NAME OF RESPONSIBLE PERSON Ramesh Harjani
a. REPORT UU	b. ABSTRACT UU	c. THIS PAGE UU			19b. TELEPHONE NUMBER 612-625-4032

**Report Title**

Design of High-Performance Survival Radios using Discrete Time Analog Signal Processing

**ABSTRACT**

In this project, we focused on the architectural and circuit-level design for a low cost, portable soldier radio with high survivability. We identified passive switched capacitor circuits as a suitable candidate for meeting these performance targets. We developed an architecture that uses a high dynamic range FFT to perform low amplitude signal detection in the presence of large jammers. Based on our analysis and modeling of non-idealities in switched capacitors, we were able to construct and simulate a sampled charge based 16 point FFT processor. The processor is able to compute the FFT of a 2GHz wideband input signal using only 1mW total power with a dynamic range exceeding 65dB without noise averaging and 90dB with noise averaging. This performance exceeds the requirements for signal detection in a typical wireless war theater communications scenario.

**List of papers submitted or published that acknowledge ARO support during this reporting period. List the papers, including journal references, in the following categories:**

**(a) Papers published in peer-reviewed journals (N/A for none)**

Number of Papers published in peer-reviewed journals: 0.00

**(b) Papers published in non-peer-reviewed journals or in conference proceedings (N/A for none)**

Number of Papers published in non peer-reviewed journals: 0.00

**(c) Presentations**

Number of Presentations: 0.00

**Non Peer-Reviewed Conference Proceeding publications (other than abstracts):**

Number of Non Peer-Reviewed Conference Proceeding publications (other than abstracts):

**Peer-Reviewed Conference Proceeding publications (other than abstracts):**

Number of Peer-Reviewed Conference Proceeding publications (other than abstracts):

**(d) Manuscripts**

Number of Manuscripts:

**Patents Submitted**

**Patents Awarded**

## Awards

### Graduate Students

<u>NAME</u>	<u>PERCENT SUPPORTED</u>
Bodhisatwa Sadhu	0.25
<b>FTE Equivalent:</b>	<b>0.25</b>
<b>Total Number:</b>	<b>1</b>

### Names of Post Doctorates

<u>NAME</u>	<u>PERCENT SUPPORTED</u>
<b>FTE Equivalent:</b>	
<b>Total Number:</b>	

### Names of Faculty Supported

<u>NAME</u>	<u>PERCENT SUPPORTED</u>	National Academy Member
Ramesh Harjani	0.01	No
<b>FTE Equivalent:</b>	<b>0.01</b>	
<b>Total Number:</b>	<b>1</b>	

### Names of Under Graduate students supported

<u>NAME</u>	<u>PERCENT SUPPORTED</u>
<b>FTE Equivalent:</b>	
<b>Total Number:</b>	

### Student Metrics

This section only applies to graduating undergraduates supported by this agreement in this reporting period

The number of undergraduates funded by this agreement who graduated during this period: .....	0.00
The number of undergraduates funded by this agreement who graduated during this period with a degree in science, mathematics, engineering, or technology fields:.....	0.00
The number of undergraduates funded by your agreement who graduated during this period and will continue to pursue a graduate or Ph.D. degree in science, mathematics, engineering, or technology fields:.....	0.00
Number of graduating undergraduates who achieved a 3.5 GPA to 4.0 (4.0 max scale): .....	0.00
Number of graduating undergraduates funded by a DoD funded Center of Excellence grant for Education, Research and Engineering: .....	0.00
The number of undergraduates funded by your agreement who graduated during this period and intend to work for the Department of Defense .....	0.00
The number of undergraduates funded by your agreement who graduated during this period and will receive scholarships or fellowships for further studies in science, mathematics, engineering or technology fields: .....	0.00

### Names of Personnel receiving masters degrees

<u>NAME</u>
<b>Total Number:</b>

---

**Names of personnel receiving PhDs**

<u>NAME</u>
-------------

Total Number:
---------------

---

**Names of other research staff**

<u>NAME</u>
-------------

<u>PERCENT SUPPORTED</u>
--------------------------

FTE Equivalent:
-----------------

Total Number:
---------------

---

**Sub Contractors (DD882)**

**Inventions (DD882)**

# Scientific Progress and Accomplishments

---

## 1. Introduction

Wireless communications has slowly become the backbone of the war fighter and it is nearly impossible to coordinate and survive modern theater interactions without wireless communications. Much of modern day research on military radio has focused on adaptability, higher bandwidths, moving to distributed architecture, jam resistance and survivability.

In this project, we focused on the architectural and circuit-level design for a low cost, portable soldier radio with high survivability. In particular, we focused on the following goals for a high-performance survival radio using discrete time analog signal processing:

- Small & portable (i.e, highly integrated)
- Low power (potentially CMOS)
- Adaptability (dynamic spectrum access)
  - Adaptable carrier frequency & adaptable signal bandwidth
- Robust to jammers
  - Ability to handle large out of band jammers
  - Ability to handle in band jammers
- Location information (may require wide signal bandwidth)
- Always connected (highest priority)
  - Always provide minimum connectivity for voice, increased signal throughput as needed

We identified passive switched capacitor circuits as a suitable candidate for meeting these performance targets. In particular, passive switched capacitors have the following advantages:

- High speed of operations
- Very low power (switching power)
- Adaptability (all linear algebra operations can be performed)
  - Adaptable carrier frequency (200MHz – 3GHz)
  - Adaptable signal bandwidth (5MHz to 25MHz)

For survival radio applications, robustness to jammers is critical. For this purpose, it is necessary to either block the jammers, or have very linear high dynamic range front-end circuitry. We had proposed a series of  $\text{sinc}^2$  and notch filters to attain the required tone suppression. However, an alternate architecture that uses a high dynamic range FFT can be used to perform low amplitude signal detection in the presence of large jammers. In the new architecture, the received signal goes to an LNTA, the output of which is sampled onto capacitors. The current domain sampling contributes a built-in anti-alias filter which can be used to filter out the large jamming tones. Following this filter, a sampled charge domain FFT is performed. The LNTA design for this project has not been completed yet but will be incorporated into the FFT design at a later time.

A very high dynamic range is required in the FFT so that it is able to function in the presence of very large jammers. In order to increase the dynamic range of the sampled charge FFT architecture, we performed an analysis of the major causes of non-linearity and noise in these circuits. These non-idealities were carefully modeled, and used for simulations. We also

developed a number of circuit techniques in order to alleviate these non-idealities, and significantly improve the dynamic range of the FFT processor. A detailed description of sampled charge processing, non-idealities and techniques to overcome them have been discussed below.

## 2. Dynamic Range in Passive Switched Capacitors

### 2.1. Sampled charge processing

Signal sampling and variable-rate analog signal processing is performed in the charge domain due to the inherent benefits of including a built-in anti-alias filter into the sampler [Carl95], robustness to jitter [Mirz08], and the ability to vary the resulting filter notches by simply varying the integration [Xu00, Yuan00, Karv06, Abid07].

Many of the benefits of the discrete time FFT architecture are based on the use of passive discrete-time charge based computations. This is best illustrated with the help of an example design. The passive switched-capacitor shown in Fig. 1 is able to operate at RF sampling speeds [Yuan00, Karv06, Abid07]. In this circuit the input signal is sampled progressively in time ( $\Phi_1 - \Phi_n$ ). After  $N$  clock periods the averaged output is sampled onto the capacitor  $C_s$ , which has previously been discharged. The complete circuit implements an  $N$ -tap FIR filter that is decimated by  $N$ . Interestingly, if the capacitor  $C_s$  is not discharged between each rotation then the circuit implements an  $N$ -tap FIR filter combined with a first-order IIR filter that is decimated by  $N$ . Note there is no “active” element (i.e., amplifier) in this circuit. The circuit consists only of switches and capacitors, so the maximum sampling rate is only dependent on the  $RC$  settling times of the switches. Additionally, the only power dissipation, other than that required for sampling the signal from the input, is due to the charging and discharging of transistor gate capacitors in a very digital-like way. As a result, a variety of functions on the sampled signal can be computed very fast and using minimal power.

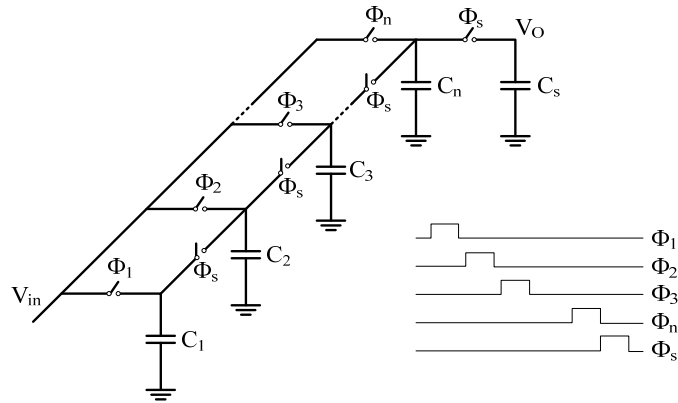


**Fig. 1: Passive switched-capacitor  $N$ -tap FIR with a decimation by  $N$**

### 2.2. Non-idealities in passive switched capacitor circuits

Several non-idealities haunt passive switched capacitor circuits. The problem of non-idealities is aggravated by the absence of a virtual ground node unlike in op-amp based switched capacitor circuits. The effect of sampling clock jitter in passive switched capacitor circuits has been analyzed. We use current mode sampling to make the circuits tolerant to sampling clock jitter [Mirz08].

Two important non-idealities: clock feed-through and charge injection, become a nuisance in the absence of a virtual ground node. Traditional circuit techniques such as bottom plate sampling

are consequently difficult to implement. Also, poor matching between  $nMOS$  and  $pMOS$  switches, and the reducing difference between  $V_{DD}$  to  $V_{th}$  in scaled technologies makes the use of transmission gate switches less effective for mitigating these non-idealities.

The noise in the system is dominated by the  $kT/C$  noise of the  $R$ - $C$  filter formed by the switch-capacitor combination. Moreover, for a multi-stage switched capacitor operation, the sampled noise voltages from one stage recombine in the later stages. These combining noise samples in a particular stage are correlated, and therefore, the final noise becomes a complicated function of the noise sampled at each stage of the switched capacitor operation.

The switch resistance (along with the capacitor's capacitance) determines the settling time constant. However, the switch resistance is inherently non-linear and input signal dependent. Consequently, in the case of high speeds of operation, incomplete settling can cause significant signal dependent errors in computations.

### 2.3. Modeling of non-idealities:

Passive switched capacitor architectures are becoming increasingly important with the scaling of technology and the newly recognized advantages of charge domain sampling. Most of the non-idealities specific to these circuits (as briefly described above) have not been well modeled. In this work, we have modeled these non-idealities and devised techniques to reduce their adverse effects on the performance of these architectures.

#### 2.3.1. Charge accumulation

Consider a switch connected between two capacitors for charge sharing. When the switch turns on, the charge required to build the channel (charge accumulation) is obtained from the two sharing capacitors. The relative amount of charge from each capacitor depends on the capacitance as well as the charge on each end of the switch. This introduces an error in each voltage at the beginning of the operation. If the capacitors have sufficient time for settling, both of them settle to the same voltage independent of this initial error. Therefore, for sufficient settling time, the charge accumulation error can be ignored. However, if the speed of operations is so high that complete settling is not feasible, a part of this initial error is retained on the participating capacitors, and needs to be modeled.

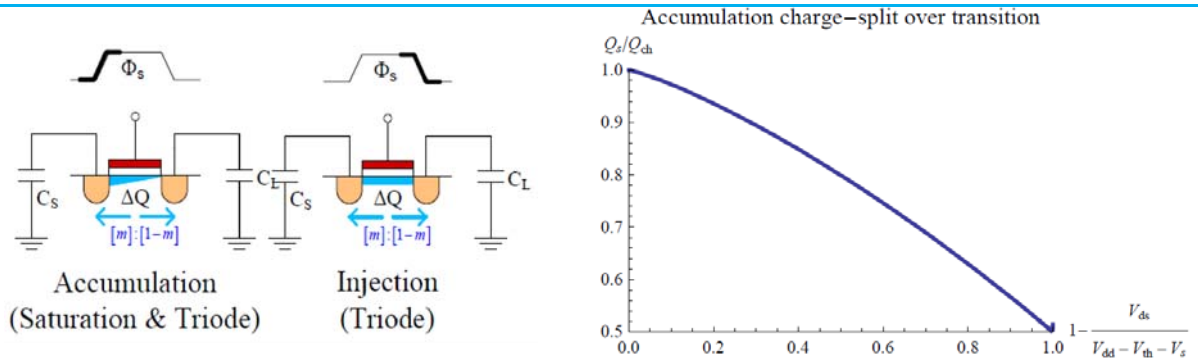


**Fig. 2: Modeling of charge accumulation and injection in switched capacitor circuits**

We modeled charge accumulation by calculating the resistance seen by each point in the channel on either side (Fig. 2). We calculated the resistance from a point in the channel to a terminal as the integral of the reciprocal of the long-channel triode charge profile versus  $V_{DS}$  from the point

to the terminal. Using the resistance seen towards each terminal, the charge split ratio for each point was calculated. We then integrated the charge split over the complete channel using the instantaneous  $V_{GS}$  voltage. Charge split in the saturation region was assumed to be 1:0, all the charge being provided by the source. The channel charge fraction from the charge splits in the triode and saturation regions were then combined to obtain the total charge split.

### 2.3.2. Charge injection

Charge injection is the channel charge dumped onto the participating capacitors at the end of a charge sharing operation. Again, it depends on the impedance looking into each end. However, since this phenomenon occurs at the end of an operation, an error is invariably introduced. For modeling the charge injection accurately for simulation purposes, we used a technique akin to that used for charge accumulation above. However, unlike in the case of charge accumulation, the  $V_{DS}$  is always very small, and the transistor remains in the deep triode region of operation throughout.

### 2.3.3. Clock feed-through

During the rising or falling edge of the clock, some charge is injected into the sharing capacitors due to the voltage divider action of the parasitic capacitance of the switch with the sharing capacitors. As a result, clock feed-through has a similar effect as charge injection and accumulation on the performance of the circuit. For a transistor switch, clock feed-through from the rising edge affects the circuit only in the case of incomplete settling, while that from the falling edge always affects the circuit.

The parasitic capacitance during the clock transition was estimated and used to accurately model the total voltage error caused. This error was taken into account in the overall model for optimization purposes. When clock feed-through cancelation schemes such as half-dummy switches were used, mismatch effects were included in the models to capture errors caused by fabrication non-idealities.

### 2.3.4. Settling

The voltage settling in a switched capacitor operation is determined by the R-C time constant of the switch-capacitance pair. In case the time available for settling is relatively small as compared to the time constant,  $\tau = RC$ , settling is incomplete.

It is important to note here that the on-resistance of the switch is variable. As a result, the time constant of the settling operation is time dependent. This needs to be accurately modeled in order to reliably capture the error caused by incomplete settling.

Consider a share and scale operation where two voltages  $V_A$  and  $V_B$  on capacitors  $C_1 = C$  and  $C_2 = C$  are shared with each other and a third stealing capacitor  $C_k = 0$  is used for scaling their sum. For a scaling factor,  $k = \frac{2}{2+C_k/C}$ , the voltages after settling should ideally be  $V_A = V_B = k \frac{v_a+v_b}{2}$ .

However, in the case of incomplete settling, the final voltage is given by:

$$V_A(t) = \overbrace{\left( \frac{v_a - v_b}{2} \right) e^{-t/\tau_d}}^{\text{Difference Settling}} + \overbrace{\left( \frac{v_a + v_b}{2} \right) k \left( 1 + \left( \frac{1}{k} - 1 \right) e^{-t/\tau_s} \right)}^{\text{Scaled Sum Settling}}$$

where,



$\tau_d$ : difference term setting	(ex. 2-point share/scale $\tau_d = RC$ )
$\tau_s$ : sum term setting	(ex. 2-point share/scale $\tau_s = RC(1-k)$ )

As can be seen from the above equations, the sum settling time constant is lower than the difference settling time constant. Therefore, in the case of incomplete settling, a larger difference settling error is caused.

### 2.3.5. Noise

Noise arises in the system from the sampling as well as the sharing operations. When a switch turns on, its noise voltage appears on the participating capacitors. When the switch turns off, this noise is sampled onto the capacitors. The resultant voltage can be modeled as a random variable added to the final output. Depending on the operation performed, the noise voltage has an expected *rms* value as follows:

$(1/2)*(kT/C)$	<i>for share</i>
$(1-k/2)*(kT/C)$	<i>for share and scale (scaling factor <math>k</math>)</i>

A larger capacitor reduces the total noise in the system. It also helps reduce other non-idealities in the system such as charge injection, accumulation, etc. However, this comes at the cost of either lower speed (larger  $RC$  time constant) or larger power consumption (same  $RC$  time constant).

The sampled noise voltages are also correlated to each other by virtue of having the same source (shared switch). This correlation is also modeled and accounted for when calculating the total, effective noise present at the output of the system.

## 2.4. Passive switched capacitor computations (additions, multiplications)

For performing any linear function, addition and multiplication operations need to be performed. Note that all passive switched capacitor operations are destructive in nature. Therefore, once an operation is performed, the input values are lost. For performing multiple operations on a single input, multiple copies of the input need to be maintained.

We have explored different techniques to perform these operations using passive switched capacitor circuits. We have compared these techniques based on their robustness to non-idealities, ease of implementation, power consumption, speed, etc. and selected suitable architectures for these computations.

### 2.4.1. Addition

#### Parallel connection

Using passive switched capacitors, addition may be performed by sharing the charges on two participating capacitors by connecting them in parallel as shown in Fig. 3. The result of this operation is the average value  $(V_1 + V_2)/2$  of the input voltages  $V_1$  and  $V_2$ , which is a scaled version of their sum operation. Also note that two copies of the output are obtained and these can be used for two independent operations later. However, the operation inherently attenuates the output by half.

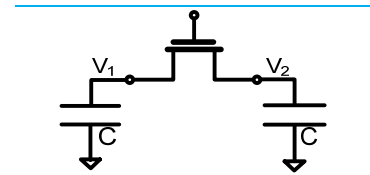


**Fig. 3: Addition using parallel connection**

From an implementation perspective, use of parallel capacitors allows the sharing of one plate (ground plate) for all the capacitors. This can greatly reduce the parasitic capacitance and resistance of the capacitor, and the area of the overall implementation.

### Series connection

An alternative technique is to connect the capacitors in series. The result of this operation is the sum  $(V_1 + V_2)$  of the input voltages  $V_1$  and  $V_2$ . In this scheme, it is possible to use slightly delayed clock phases for the top and bottom plate switches in order to make the charge injection independent of the input voltage [Guil05]. However, in this latter technique, switches are required both on the top and bottom plate, thereby increasing the power consumption in this circuit. Also, the two switches placed in series halves the speed of this circuit for identical switch sizes. Moreover, only one output (which can be used for exactly one subsequent operation) is obtained.

Considering the improvements in speed, power, area, and the availability of two outputs for further operations, the parallel connection scheme was selected for further analysis.

## 2.4.2. Multiplication

### Charge stealing

Multiplication in the charge domain can be performed by scaling the voltage on a capacitor using a share operation with another known capacitor (stealing capacitor). The charge on the stealing capacitor is not utilized later. The overall operation causes a sub-unity scaling on the original value. The scaling factor for a capacitor of value  $C$  and a stealing capacitor of value  $C_k$  is given by  $k = C/(C+C_k)$ .

Fig. 4 shows a scaling operation using a stealing capacitor of size  $C_k$  with no initial voltage on it. After the sharing operation, the final value on the capacitor with initial value  $V_0$  becomes  $V_0 \cdot C/(C+C_k)$ .  $C_k$  can be chosen appropriately to obtain a particular scaling factor.

Note that though this technique is capable of performing both sub-unity scaling and multiplication with a known attenuation, at least one of the operands needs to be known in advance for this implementation. In case variable capacitors are utilized, dynamic operands can also be used.

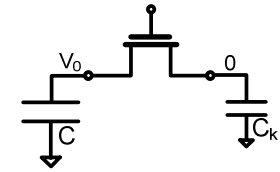


**Fig. 4: Addition using parallel connection**

### PWM

Another technique to perform multiplication using passive switched capacitors is to modulate the turn on time of the switch and perform an incomplete share operation with a fixed stealing capacitor. The duration of the operation determines the multiplication factor. It is possible to multiply two unknown operands using this technique. However, considering the non-linearity in the resistance and the share operation, the errors caused by this technique make it unusable. However, the concept can be used to devise another PWM scheme which allows complete settling thereby making it more reliable.

In this modified technique, the switch can be turned on using a sequence of randomly placed pulses and sharing the capacitor charge using a small stealing capacitor for each clock cycle. The stealing capacitor is discharged at the end of each cycle. Complete settling is allowed in each cycle. The total number of on-pulses determines the amount of scaling. Maximum scaling is

obtained when all the clock cycles have on pulses, while no scaling is obtained when all the clock cycles have off pulses.

Although this technique is relatively accurate, and is able to handle dynamic operands, it is slow and consumes more power than the charge stealing technique. Also, depending on the accuracy required, the attenuation is considerable.

### Current domain

If the charge is converted to the current domain, a single, variable-duration pulse PWM scheme can be used to perform multiplication. Also, multiplication would not entail an inherent attenuation. However, the technique is very power hungry, and the accuracy of the transconductance amplifier that translates from charge to current domain needs to be very very high.

We have focused on the charge stealing concept for performing multiplications due to their low power characteristics. For most linear algebra problems, multiplication using fixed coefficients is sufficient, and this technique lends itself easily to such applications.

## 2.5. Circuit techniques to overcome non-idealities

A number of circuit techniques were devised to tackle the non-linearities discussed above in the addition and multiplication operations. The techniques of parallel charge sharing for addition, and charge stealing for multiplication, have been considered when devising these techniques.

### 2.5.1. Switching schemes

For reducing the attenuation, different sharing techniques can be used. 2 capacitors are shared as shown in Fig. 3. We can combine a share followed by scaling into a single operation by connecting 3 capacitors (2 with input samples and 1 empty) and sharing their charges. This can be performed in different ways using 2

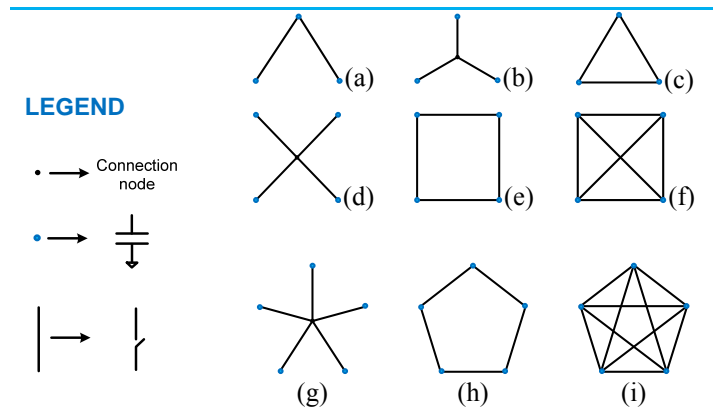


**Fig. 5: Different switching schemes for use in the FFT processing engine**

switches or 3 switches as shown in Fig. 5(a,b,c). Additionally, it is possible to reduce the  $kT/C$  noise contribution of the overall structure by using 3 appropriately sized switches in the scheme of Fig. 5(c). Similarly, different schemes may be used for sharing 4 and 5 capacitors for scaling by complex factors of the form ' $c + cj$ ' (see Section 2.4 for complex operand scaling techniques) as shown in Fig. 5(d,e,f,g,h,i). While some schemes (Fig. 5(b,d,g)) ensure symmetry, others (Fig. 5(a,e,h)) offer faster computations for the same/lower number of switches as compared to Fig. 5(b,d,h). Some schemes (Fig. 5(c,f,i)) provide both speed and symmetry at the cost of a larger power dissipation. Also, different schemes, with their appropriate switch sizes, provide different trade-offs with regard to noise contribution, charge injection error, clock feed-through error, etc. Based on the models we have developed the choice of specific switching schemes to improve the noise, speed and non-linearity of the overall system was optimized. A

summary of the trade-offs (numbers are relative to a single switch share operation in Fig. 3) is shown in Table 1 below.

**Table 1: Summary of trade-offs among different switching schemes**

Switching scheme used	$\tau_s$ (RC)	$\tau_d$ (RC)	$P_{sw}$	$P_{sw}(\tau_s + \tau_d)/N$	Noise ( $kT/C$ )
2 switch (Fig. 5(a))	1	1	2	2	$1-k/2$
3sw star (Fig. 5(b))	2	1	3	4.5	$1-k/2$
3sw triangle (Fig. 5(c))	1	0.33	3	2	$1-k/2$
3sw noise optimum (Fig. 5(c))	1	0.58	2.37	1.87	$0.87-k/2$
4 switch (Fig. 5(d))	1	1	4	2	$1-k/4$
Pentagon (Fig. 5(h))	1	0.5	5	1.88	$1-k/4$
10 switch (Fig. 5(i))	1	0.2	10	3	$1-k/4$
10sw optimum (Fig. 5(i))	1	0.45	5.85	2.12	$0.71-k/4$

### 2.5.2. Wire swapping

As we discussed previously, there is a clear trade-off between power and speed for the charge based FFT engine. However, it is possible to exploit the presence of multiple copies, the differential nature of the design, and good matching accuracy to speed up the processing by using a faster clock than the design allows.

To understand this, let us take an example, as shown in Fig. 6. The figure shows a pair of capacitors ((1+) and (2+)) sharing their charges and settling to a final value over time. Another pair of capacitors ((1-) and (2-)) in the differential implementation are sharing their charges similarly. If the voltages are not allowed to completely settle, the final differential outputs ((1+) – (1-)) and ((2+) – (2-)) will be incorrect. However, if we swap one set of voltages and instead compute the outputs as ((1+) – (2-)) and ((2+) – (1-)), the differential outputs will still be correct.

Since the time constant for differential settling is higher than that for common mode settling, incomplete settling using wire swapping can be very advantageous.

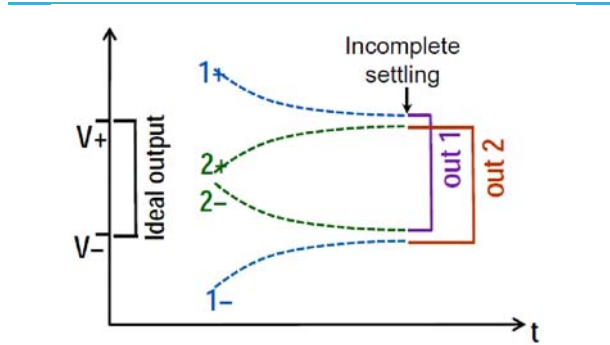


**Fig. 6: Incomplete settling for high speed processing**

### 2.5.3. Noise reduction

As discussed earlier, the correlation between sampled noise copies can be utilized to cancel out a part of the noise in operations. Also, the switch scheme (number of switches, their connectivity, and their relative sizes) affect the total noise sampled onto the participating capacitors.

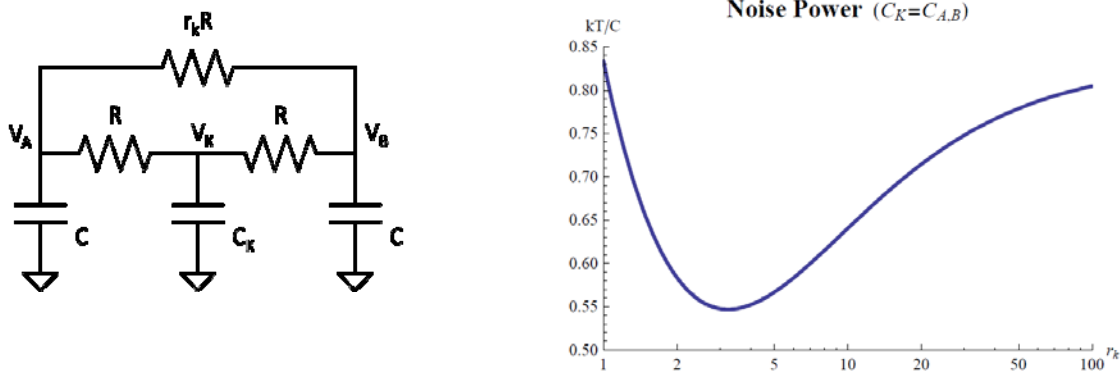


**Fig. 7: Share and scale scheme using three switches for noise optimization**

For example, for a share operation (voltage averaging) between two capacitors, using three switches instead of two reduces the total noise sampled onto the capacitors. This is shown in Fig. 7. The switches are represented by their average turn on resistances. For optimal noise performance, two switches need to be equal in size while the third switch has a size smaller than these. Plotting the total noise power for different sizes of the third switch, we find an optimal switch size.

Similar schemes have been devised for the more elaborate sharing techniques discussed earlier. The performance of optimal switching schemes has been summarized in Table 1.

In addition to this, the correlation among the noise samples can be used to reduce their effect by appropriately sharing capacitors during a later operation in a sequence. Methods to perform this have also been devised.

#### 2.5.4. Variable selection

A number of variables appear in the optimization problem. These variables affect the speed, power, and accuracy of the passive switched capacitor circuitry in complex ways. The design entails multiple trade-offs, as summarized in Table II. The operation speed (clock frequency) of the design determines the  $R_{on}C$  constant of the switch-capacitor combination. The  $R_{on}$  of the switch is again dependent on the switch size ( $W_{sw}$ , which determines  $C_{sw}$ ) and  $V_{DD}$ . Consequently, for a given sampling capacitance,  $C$ , different combinations of  $V_{DD}$  and  $C_{sw}$  ( $W_{sw}$ ) can be used to provide a particular operation speed. Among these, we optimize and select the switch size and  $V_{DD}$  that provides the lowest power for each stage. Programmable level shifters

**Table II: Trade-offs in charge domain FFT design**

Variables	Increase	Decrease
$C$	SNR, Charge-injection, Charge-accumulation, Clock feed-through	Power, Speed
$W$	Speed, Non-linear $R_{on}$	Power, Charge-injection, Charge accumulation, Clock feed-through
$V_{DD}$	Speed, Non-linear $R_{on}$	Power
$V_{sw}$	SNR	Non-linear $R_{on}$

can be utilized for the required  $V_{DD}$  scaling.

There are similar trade-offs between the speed, noise and non-linearity of the system. Increasing the capacitance improves the noise floor, which for our sampled data system is dominated by  $kT/C$  noise. It also improves the robustness of the system to charge-injection and clock feed-through errors. However, a larger capacitance degrades the  $R_{on}C$  constant and slows down the system. Increasing the input voltage swing ( $V_{sw}$ ) improves the signal-to-noise ratio. However, this introduces significant non-linearities in the switch on-resistance. It is possible to increase  $V_{DD}$  to reduce this non-linearity and improve the speed, but at the cost of a larger power dissipation (quadratic dependence).

## 2.6. FFT computation

The DFT is mathematically defined as:

$$S_k = \sum_{n=0}^{N-1} s_n e^{-\frac{2\pi jkn}{N}}.$$

The constituent functions in this definition are multiplications by sub-unity twiddle factors and additions of the results. While these functions, especially the former, can be expensive (high power) in the digital domain, they can be computed inexpensively using passive switched capacitor circuits. We perform additions in the charge domain by sharing the charge on multiple capacitors as shown in Fig. 8(a) (an average is a scaled sum), and performing sub-unity scaling by stealing away charge from a capacitor onto another capacitor as shown in Fig. 8(b). Scaling with complex twiddle factors can be performed using a combination of the addition and scalar multiplication operations, as shown in Fig. 8(c). Note that 2 copies of each sample are required for complex multiplications.

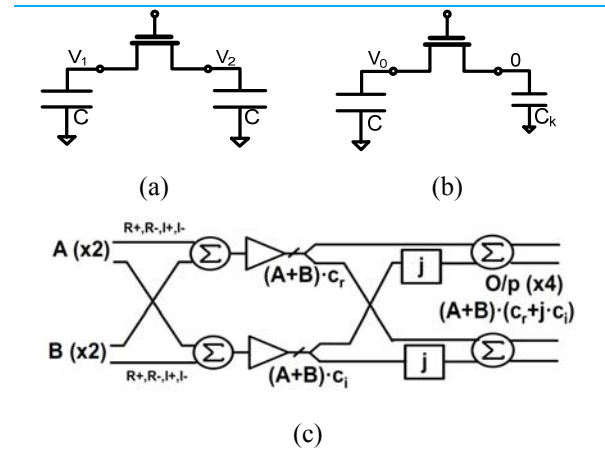


**Fig. 8: Addition and multiplication using passive switched capacitor circuits**

(a)  $V = (V_1 + V_2)/2$

(b)  $V = V_0/(C + C_k)$

(c) **Complex multiplication:**  $Y = (A+B) \cdot (c_r + j \cdot c_i)$ ,  $A$  &  $B$  are inputs;  $w = (c_r + j \cdot c_i)$  is a complex twiddle factor

The Fast Fourier Transform (FFT) algorithm can be used to reduce the number of computations. The input signal is first sampled onto a set of capacitors. These can then be used to perform all computations in the butterfly using the different charge sharing operations described previously. All calculations are performed on the original sampled charge using in-place computations, and the original values are therefore destroyed. The operations being destructive, multiple copies of the sampled inputs are required in order to perform multiple operations on the same input sample. Within a butterfly, each input is operated on twice (2 copies), and each operation is a complex add and multiply (2 more copies). Therefore, 4 copies of each value are required at all stages in the FFT computation. Although the presence of multiple copies is an overhead in this technique, it becomes negligible when compared to the orders of magnitude improvement in power savings. Also, the presence of multiple copies can be exploited to obtain other benefits as discussed earlier.



## 2.7. Detailed FFT modeling and results

Based on the mathematical models we developed for the different performance metrics as a function of the design variables, we designed, optimized and simulated a 16 point FFT engine in Matlab. Dynamic range, speed, and power were the major optimization parameters emphasized. Results from the example design based on the modeling and optimization described above are shown in Fig. 9. The modeling is based on a 65nm technology node. The red lines represent results from different runs with a tone in a particular FFT bin. The average of the resultant magnitudes forms the envelope shown by the yellow line. This is the average dynamic range that can be obtained from the system (about 65dB, equivalent to 11 bits of digital resolution). In case multiple measurements can be taken, the complex outputs can be averaged to reduce the effective noise in the output. The blue line represents an average of 256 independent runs. Assuming that the noise is no longer the dominant source of error, the blue curve then represents the non-linearity floor in the overall system ( $\sim 90$ dB, or 15 bits of resolution). This dynamic range is sufficient to block out jammers in a typical war theater for survival radio applications.

The FFT engine is able to operate at a speed of 5GS/s with a 2GHz input signal bandwidth. The total simulated power consumed by the FFT processor is 0.5mW for sampling and 0.5mW for processing and 0.5mW for sampling.

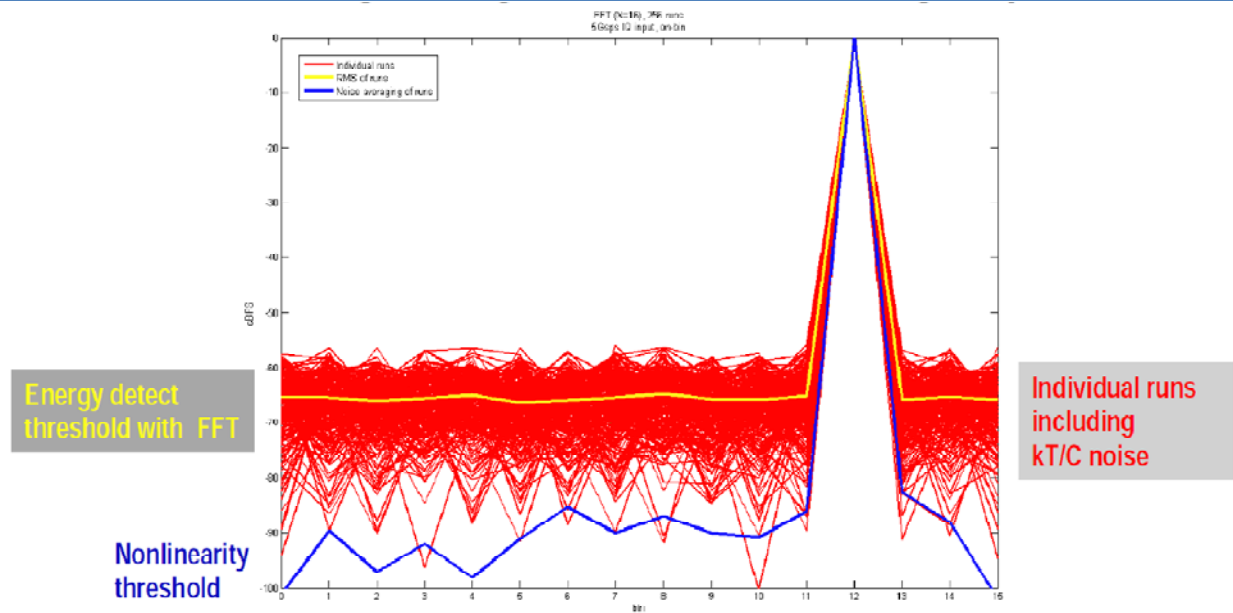


Fig. 9: Matlab simulations of a full 16-point FFT core

## 3. Conclusions

Sampled charge passive switched capacitor circuits were identified as suitable candidates for survival radio applications. High speed, power, and dynamic range were recognized as critical parameters, and a detailed analysis was performed to evaluate the effect of the circuit variables on these parameters based on a 65nm CMOS technology node. Based on the analysis, models were developed, and an optimization framework was designed to optimize these parameters. We were able to design and simulate a 16 point FFT processor that is able to process a 2GHz

wideband input signal using only 1mW total power with a dynamic range exceeding 65dB without noise averaging and 90dB with noise averaging. This dynamic range is sufficient for tackling very large jammers in a typical wireless war theater communications scenario with friendly and adversarial jammers, multipath fading and difficult NLOS operation.

## 4. Bibliography

- [Abid07] Asad A. Abidi, "Evolution of the software-defined radio (SDR) receiver," VLSI Circuits Symposium tutorial, 2007.
- [Guil05] N.J. Guilar, P-K Lau, P.J. Hurst and S. H. Lewis, "A 200 MS/s Passive Switched-Capacitor FIR Equalizer Using a Time-Interleaved Topology," in Proc. IEEE Custom Integrated Circuits Conference, 2005.
- [Karv06] Sami Karvonen, "Charge-domain sampling of high-frequency signals with embedded filtering," Ph.D. Thesis, University of Oulu, 2006.
- [Mirz08] A. Mirzaei, S. Chehrazi, R. Bagheri and A.A. Abidi, "Analysis of first-order anti-aliasing integration sampler," IEEE TCAS I, vol 55, No 10, Nov, 2008.
- [Xu00] Gang Xu and Jiren Yuan, "Comparison of charge sampling and voltage sampling," 2000. Proceedings of the 43rd IEEE Midwest Symposium on Circuits and Systems, Vol 1, 2000.
- [Yuan00] Jiren Yuan, "A charge sampling mixer with embedded filter function for wireless applications," IEEE International Conference on Microwave and Millimeter Technology Proceedings, 2000.